CHAPTER 5

MODEL OF VEHICLE/TRACK SYSTEM DYNAMICS

In this chapter the development of the vehicle/track model to be used in the Dynamic Track Deterioration Prediction Model is described. Firstly, the rail support model is described, followed by a detailed description of the excitation model which consists out of the vertical space curve as well as spatial track stiffness variations. As the choice of assumptions and simplifications in the mathematical model of the vehicle is important in the development of the model, the basic philosophy in this respect is outlined before describing the development of the mathematical vehicle/track model.

The first model that is described is a two degree-of-freedom model. This model was used to do a basic analysis of the influence of spatial track stiffness variations on the dynamic behaviour of such a model. After considering a number of alternative vehicle/track models the reasons for arriving at the eleven degree-of-freedom model become apparent. The validation of the eleven degree-of-freedom model is given in Chapter 7.

5.1 TRACK SUPPORT MODEL

Although a discrete support appears to be more representative of track supported by discrete sleepers on a nonlinear and spatially varying flexible foundation, continuous support models are valid for calculating the dynamic response of the track at frequencies below 500 Hz (Knothe and Grassie, 1993). The simplest representation of a continuous elastic foundation is the Winkler foundation model.

In this model the rail is represented by an infinite, uniform, Euler-Bernoulli beam supported by a continuous damped, elastic Winkler foundation. The effective mass of the sleepers is distributed uniformly and added to the mass of the rail (Winkler, 1867; Winkler, 1875; Hetényi, 1946; Fastenrath, 1977; Esveld, 1989; Li and Selig, 1995). Winkler's hypothesis states that at each rail support the compressive stress is proportional to the local compression, that is

$$\sigma = C_f y \tag{5.1}$$

where

σ = local compressive stress on the support,

y = local deflection of the support, and

C_f = foundation modulus [N/m^3].

Based on the Winkler theory, the track modulus, u, which represents the overall stiffness of the rail foundation (that is sleepers, rail pads, ballast, sub-ballast, and subgrade), is defined as the supporting force per unit length of rail per unit deflection. Thus

$$u = \frac{q}{y} \tag{5.2}$$

with q the vertical rail foundation force per unit length.

The track stiffness itself is defined as

$$k = \frac{P}{y} \tag{5.3}$$

with P the concentrated force applied to the rail.

The difference between the track stiffness and the track modulus is that the track stiffness includes the rail stiffness, EI, whereas the track modulus represents only the remainder of the superstructure and the substructure. The various components of ballasted track are shown in Figure 5.1.

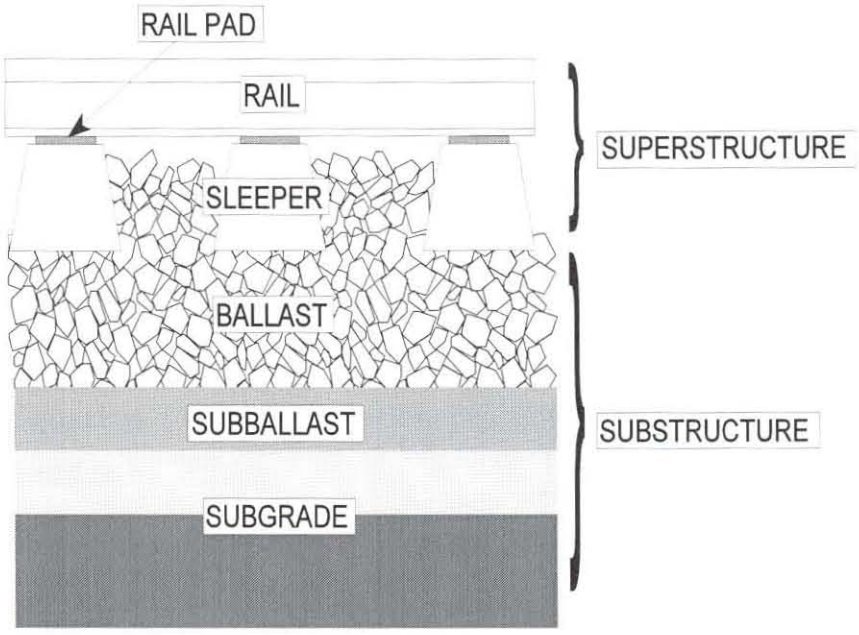

Figure 5.1: Components of ballasted track.

The linear differential equation of the beam-on-elastic foundation model is given as:

$$EI \frac{d^4y}{dx^4} + uy = 0 \tag{5.4}$$

where

E = Young's modulus of rail steel,

I = rail moment of inertia about the horizontal axis,

y = incremental track deflection, and

x = distance from the applied load.

Solving Equation (5.4), the deflected shape of the track is

$$y = \frac{P}{2uL_c} e^{-x/L_c} [\cos(x/L_c) + \sin(x/L_c)] \tag{5.5}$$

The characteristic length, L_c, is defined as

$$L_c = \sqrt[4]{\frac{4EI}{k}} \tag{5.6}$$

Substituting Equation (5.3) and (5.6) into Equation (5.4), the relationship between the track modulus and the track stiffness is given as

$$u = \frac{(k)^{4/3}}{(64EI)^{1/3}} \tag{5.7}$$

Re-writing Equation (5.7), the relationship between track stiffness and track modulus is found to be

$$k = \frac{2u}{\sqrt[4]{\frac{u}{4EI}}} \tag{5.8}$$

As illustrated in Figure 5.2, the rail support can also be nonlinear. The slope of the line between 0 and 32.5kN gives an indication of the voids between the sleepers and the ballast in the influence length of the wheel load (Ebersöhn *et al.*, 1993). The 32.5kN load is referred to as the seating load. For higher wheel loads the load deflection relationship is linear in most cases although in some cases stiffening of the track is found. This phenomenon makes it more complex to determine the deflection basin especially if the track stiffness also varies from point to point along the track.

To analyse the effect of wheel loads on the shape of the track deflection basin, and on the distribution of the wheel loads across a number of adjacent sleepers when the track has a spatially varying nonlinear support stiffness, a track model using elastic Euler-Bernoulli beams supported on a nonlinear discrete support has to be used. The rail in such a model is thus modelled by a finite element flexible beam and the structure is approximated as an assemblage of discrete elements interconnected at their nodal points. To find the solution to the nonlinear structural response, a load stepping procedure like the Newton-Raphson iteration procedure can be used. This

procedure is stable and converges quadratically although the stiffness matrix has to be inverted during each iteration.

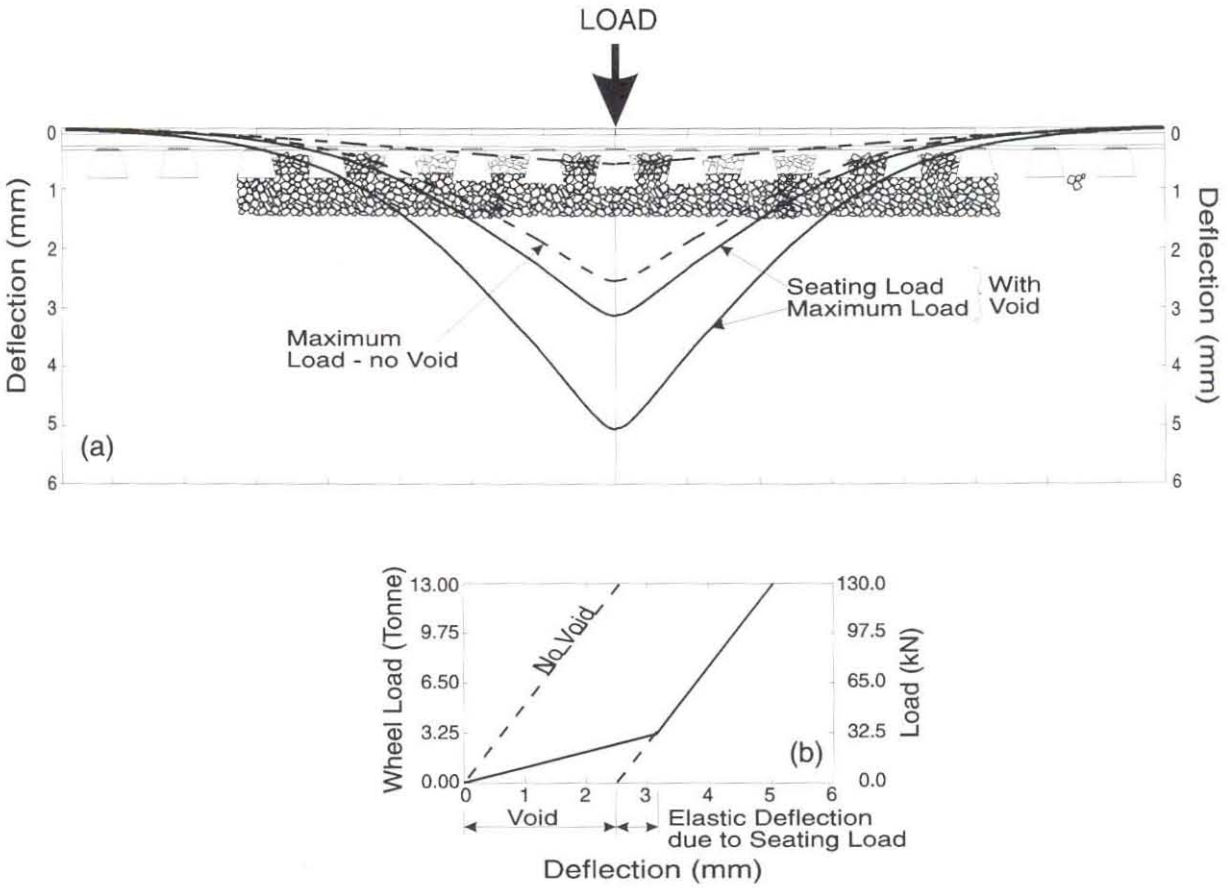

Figure 5.2: Track deflection basin.

In 1995, Moravčík made an analysis of rail on nonlinear discrete elastic supports. According to Moravčík the theoretical model of the rail as a beam on a continuous elastic foundation provides a basis for track design and stress analysis of the track components. However, due to on-track tests which revealed that the relationship between the vertical rail deflection and the wheel load is generally nonlinear, a different approach was required and a nonlinear finite element program was used to solve the problem. The nonlinear relationship between the wheel load and the vertical displacement of the sleeper was approximated by a bilinear spring, supports

with gaps, or a piecewise linear spring characteristic. Such a nonlinear analysis of the deflection basin provided a better picture of the rail behaviour, specially under locally poor track conditions where a large reduction in support resistance could be the major cause of overstressing in the track structure. A standard linear analysis generally underestimates the stresses in the track structure.

In this research a continuous one-layer pseudo-static track support model is used, but allowing the track stiffness to vary with time according to the instantaneous local track stiffness values underneath each wheel on both the left and the right hand rail of the track. Track damping is assumed to be constant along the track.

5.2 TRACK INPUT

The vehicle/track model is excited by the vertical space curve of the track as well as spatial vertical track stiffness variations. The excitation model is a moving excitation model, that is the vertical space curve and the stiffness variations are effectively pulled through under the wheelset.

If the track stiffness is linear, the vertical track profile variations can simply be multiplied by the track stiffness to determine the effective force input. However, if the track stiffness is nonlinear, an effective linearised loaded track stiffness, k_2, and an effective loaded track deflection, y_s, as shown in Figure 5.3 has to be used. Using the nonlinear track stiffness as measured at each sleeper, the following procedure is used to derive the effective linearised loaded track stiffness.

Let P_s be the static wheel load and

$$\Delta P = \delta P_s \tag{5.9}$$

where δ is the dynamic wheel load increment. The wheel load increment is obtained from the prevailing dynamic wheel load as measured by the load measuring wheelset. If such a value is not available a good estimate is 0.3.

Using cubic-polynomial interpolation, the values y_{s1} and y_{s2} are found at $(P_s-\Delta P)$ and $(P_s+\Delta P)$ respectively. With these values available, the effective linearised loaded track stiffness is defined as

$$k_2 = \frac{P_s}{y_{s2} - y_{s1}} \tag{5.10}$$

and the static track deflection is defined as

$$y_s = \frac{y_{s2} + y_{s1}}{2} \tag{5.11}$$

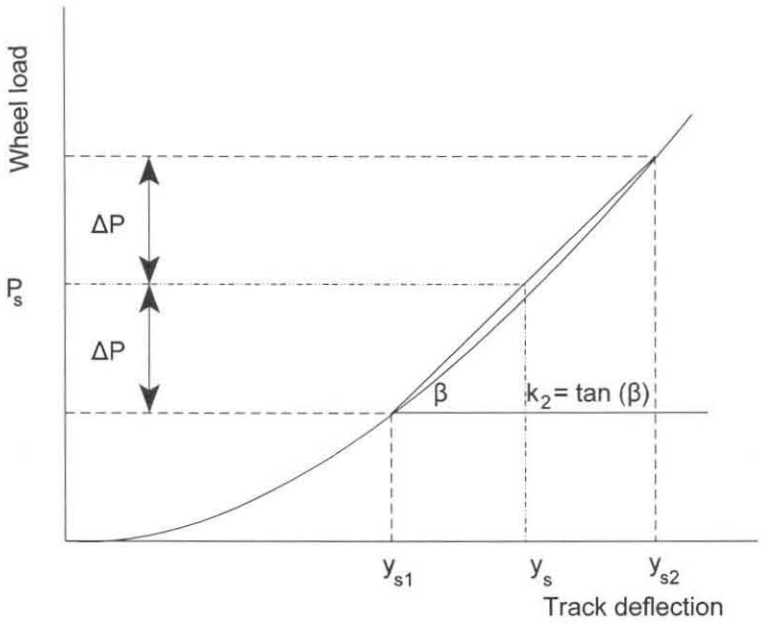

Figure 5.3: Effective linearised loaded track stiffness.

Linearisation is thus done over a range of static wheel load plus the dynamic increment. Figure 5.3 clearly shows that only a minimal deviation occurs between the linear approximation and the measured nonlinear stiffness. Note that due to the static load at a particular sleeper that is supported by a nonlinear track stiffness, the sleeper is deflected by a certain amount y_s. Would there be no spatial variation in the track stiffness, this would not be important, but as there are continuous

variations in the track stiffness, these deflections due to static or dynamic loading, vary as a function of the specific spatially varying load-deflection curve. An example is given in Figure 5.4. These varying deflections are added to the unloaded vertical space curve to obtain the effective loaded track geometry profile. This profile is then multiplied by the effective linearised loaded track stiffness at a particular point in the track to give the required input force to the mathematical model of the vehicle/track system. An effective linearised loaded track stiffness and loaded geometry profile which depends on the static and dynamic wheel load is thus obtained.

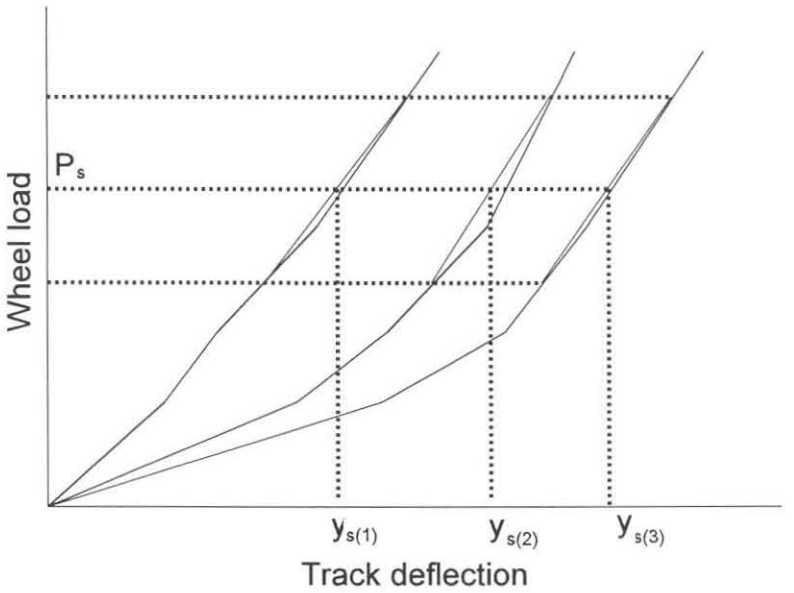

Figure 5.4: Varying static track deflections.

5.3 VEHICLE MODEL

Although a range of vehicle models are available to the rail vehicle dynamicist, unique requirements make it necessary to develop more suitable models from time to time. Such a unique application is the development of the Dynamic Track Deterioration Prediction Model that is to be used to predict and show the important relationship between spatially varying track stiffness and track deterioration.

Before proceeding with the development of the vehicle/track model that is to be incorporated in the Dynamic Track Deterioration Prediction Model, the basic philosophy behind the assumptions and simplifications in the development of vehicle models is given.

When developing a mathematical model of a railway vehicle it is important to have accurate data for parameters such as masses, stiffnesses, damping rate, friction levels etc. Furthermore it is up to the experienced railway vehicle dynamicist to make an informed judgement as to what level of detail to include in the model. Provided that realistic sensitivity studies have been done during the development of a new model to ensure that the parameters used are either not critical or at least reasonably realistic, calculated trends and comparisons can give a good insight into dynamic rail vehicle behaviour.

As the objective of this thesis is to predict the dynamic interaction between the vehicle and the track, and not the dynamic behaviour of the vehicle alone, the development of the vehicle model is done in terms of the development of the total vehicle/track system model.

5.4 VEHICLE/TRACK MODEL DEVELOPMENT

This section discusses the development of the vehicle/track model. The first model that is described is a two degree-of-freedom model. This is followed by a set of alternative models which systematically strive to adequately simulate the dynamic behaviour in the vehicle/track system. Finally, an eleven degree-of-freedom vehicle/track model is described. This model is sufficient for investigating the relationship between spatial track stiffness variations and track deterioration. For the interested reader some background information on dynamic modelling of a simple one degree-of-freedom system is given in Appendix D.

5.4.1 Two Degree-of-Freedom Vehicle/Track Model

To be able to gain a better understanding of the dynamic interaction between a vehicle and the track, a *two degree-of-freedom model* as shown in Figure 5.5 was initially developed. The two degree-of-freedom model was used to determine the dynamic wheel loads in the vehicle/track system due to a nonlinear and spatially varying track stiffness (Fröhling *et al.*, 1996a). By restricting the number of degrees of freedom to be investigated, a simpler understanding of the problem was formed and the emphasis was placed on effects due to the nonlinear spatially varying track stiffness.

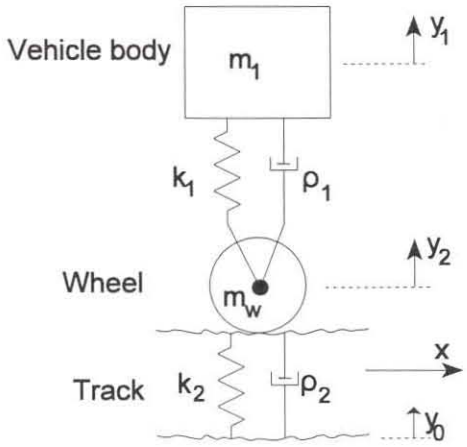

Figure 5.5: Two Degree-of-Freedom Vehicle/Track Model.

In this simplified model the following assumptions were made:

- The effect of the primary suspension of the vehicle was neglected.
- The stiffness and damping of the secondary suspension of the vehicle was assumed to be linear.
- A continuous one-layer track support model was used.
- The mass of the vehicle body represents one eighth of the sprung mass of the vehicle as this is the mass that is effectively carried by each of the eight wheels of the vehicle.
- Both the vehicle and the wheel are assumed to be rigid bodies.

The following nonlinear equations of motion describe the dynamic behaviour of the two degree-of-freedom vehicle/track model.

$$m_1\ddot{y}_1 + \rho_1\dot{y}_1 + k_1y_1 - \rho_1\dot{y}_2 - k_1y_2 = 0 \tag{5.12}$$

$$m_w\ddot{y}_2 + (\rho_1 + \rho_2)\dot{y}_2 + (k_1 + k_2(y_2,x))y_2 - \rho_1\dot{y}_1 - k_1y_1 - k_2(y_2,x)y_0 = 0 \tag{5.13}$$

$$k_2(y_2,x) = f(y_2,x) \tag{5.14}$$

The instantaneous value for the track stiffness, k_2, is obtained from a bi-variant cubic polynomial interpolation in the two-dimensional data set of measured track stiffness values. The value of the track stiffness is also dependant on the prevailing static wheel load.

To solve the system of equations as given by Equations (5.12) to (5.14), the derivatives in the differential equations are replaced by finite central difference approximations (Levy and Wilkinson, 1976). In the approximation the derivative of y with respect to t is defined at $t=t_0$ by

$$\left(\frac{dy}{dt}\right)_{t=t_0} = \frac{\Delta y}{\Delta t} = \frac{y_1 - y_{-1}}{t_1 - t_{-1}} = \frac{y_1 - y_{-1}}{2\Delta t} \tag{5.15}$$

Likewise, a similar approximation can be made for the acceleration which is the second derivative:

$$\left(\frac{d^2y}{dt^2}\right)_{t=t_0} = \frac{y - 2y_0 + y_{-1}}{(\Delta t)^2} \tag{5.16}$$

By introducing these approximations, the derivatives in the equations of motion can be replaced by the differences between successive positions taken by the mass at successive increments in time. These differences are known as finite differences because they are separated by finite time increments.

Equations (5.12) and (5.13) are thus re-written as:

$$m_1\left(\frac{y_{1(1)}-2y_{1(0)}+y_{1(-1)}}{(\Delta t)^2}\right)+\rho_1\left(\frac{y_{1(1)}-y_{1(-1)}}{2\Delta t}\right)+k_1y_{1(0)}-\rho_1\left(\frac{y_{2(1)}-y_{2(-1)}}{2\Delta t}\right)-k_1y_{2(0)}=0 \qquad (5.17)$$

$$m_w\left(\frac{y_{2(1)}-2y_{2(0)}+y_{2(-1)}}{(\Delta t)^2}\right)+(\rho_1+\rho_2)\left(\frac{y_{2(1)}-y_{2(-1)}}{2\Delta t}\right)+(k_1+k_2(y_{2(0)},x))y_{2(0)}-\rho_1\left(\frac{y_{1(1)}-y_{1(-1)}}{2\Delta t}\right)-k_1y_{1(0)}-k_2(y_{2(0)},x)y_0=0 \qquad (5.18)$$

The three simultaneous nonlinear equations are solved at each time step, using the Newton-Raphson algorithm. Having obtained the displacement values $y_{1(1)}$ and $y_{2(1)}$, and the instantaneous track stiffness, the values $y_{1(2)}$ and $y_{2(2)}$ are found in terms of the already calculated values. This process of finding the new displacement based on knowledge of the two previous displacements is known as a step-by-step process of integration. The procedure is simple in concept, but can, with repetitive application, yield the complete time history of the behaviour of the system. By adjusting the size of the time step Δt, the desired accuracy can be obtained. Convergence with a nonlinear set of equations is readily obtained using this approach. This numerical solution technique was used in a computer program which was developed to solve the system of equations of the two degree-of-freedom vehicle/track model at each consecutive time step using the instantaneous information on track geometry and track stiffness variations.

The two degree-of-freedom model was used to simulate both an empty and a loaded vehicle, both alternatively equipped with a low and a high secondary damping, running over a section of irregular track (Fröhling *et al.*, 1996a). Under these conditions, the vertical acceleration of the vehicle body and the dynamic loading of the track was analysed as a function of the vertical space curve of the track and an infinite track stiffness, the vertical space curve of the track and a constant track stiffness, no track geometry irregularities and only a spatially varying track stiffness, and spatially varying track stiffness superimposed on the vertical space curve of the track. From simulations over single vertical track geometry irregularities, it was found that it is not the nonlinearity of the track stiffness in itself that causes a dynamic input, but the spatial change in track deflection under a given load.

Using the two degree-of-freedom model and comparing the results to those measured during on-track tests, it became clear that the model is not able to simulate the low frequency dynamic behaviour that originates from the rolling motion of the wagon body. These motions were dominant in the measured results. Furthermore, the model was not able to simulate the difference in track input between the left and the right rail. Hence, further model development was required.

5.4.2 Alternative Vehicle/Track Models

After realising the limitations of the two degree-of-freedom vehicle/track model, the search for a more appropriate vehicle/track model started. The first step was to *incorporate the load sensitive damping of the secondary suspension* into the two degree-of-freedom model by using Equations (B1) to (B3) given in Appendix B. This was done because of the nonlinear displacement that was measured across the secondary suspension during the on-track tests, and its influence on the force transmitted through the secondary suspension and thus also the resultant force between the wheel and the rail.

The next step was to *include the rolling motion* of the wheelset and the vehicle body. This was done using a two dimensional four degree-of-freedom model with varying track input between the left and the right rail. This model was tested with and without load sensitive frictional damping. Comparing its results to those measured on track, it became clear that this model was unable to simulate the coupling between the dynamic wheel load in the front of the vehicle and that at the trailing end that occurs due to the distance based track input. To include this effect, the *pitching motion* of the vehicle was included. This resulted in a seven degree-of-freedom model.

At this stage the magnitude of the dynamic wheel load and the vertical displacement across the secondary suspension was still not representative of the measured results. Patterns were however becoming similar.

5.4.3 Eleven Degree-of-Freedom Vehicle/Track Model

The next step was to include the *vertical stiffness and damping of the primary suspension*, increasing the degrees-of-freedom of the model to eleven. At this stage the vehicle/track model was still simulating a two-axle vehicle and not a two-bogie vehicle as used during the on-track tests. The following was however done to include some influence due a bogie with two wheelsets on the dynamic behaviour of the vehicle/track system.

- To get the correct dynamic track deflection, the mass and the inertia of the two wheelsets of the bogie were added together to create a wheelset with twice the mass of the actual wheelset. The two wheelsets were thus seen to be close enough to one another to act as one inertial system and the exact behaviour of the unsprung mass was thus of secondary importance.
- To simulate the vertical space curve of the track as seen by a bogie, the average between the vertical space curve at the leading and the trailing axle on one side of the bogie was calculated at any point in time and used as excitation input. This made it possible simulated the effect the side frames have on averaging the force input to the secondary suspension.
- To compensate for the fact that only one and not two wheels are in contact with the track on one side of the bogie, the track stiffness as observed at any point in time at the leading and the trailing wheel on one side of the bogie was added together to simulate the fact that a quarter of the vehicle is effectively being supported by two times the track stiffness.

The simulated results were checked against results obtained with the multi-body simulation program MEDYNA (Schielen, 1990). In the MEDYNA model the side frames of the bogies were modelled as separate bodies. The results showed that the approximation described above was sufficient to predict the magnitude of the dynamic wheel load, the vertical displacement across the secondary suspension, and the dominant frequencies in the system. The validation of the eleven degree-of-

freedom vehicle/track model is done in Chapter 7. A complete list of assumptions and the overall motivation for these assumptions is also given in Chapter 7.

The vehicle/track model was thus developed in close conjunction with experimental results. In particular the patterns and the magnitudes of the vertical displacement across the secondary suspension and the dynamic wheel loads were used for this purpose. Fault finding and sensitivity studies were also part of the development process. A schematic of the eleven degree-of-freedom vehicle/track model is shown in Figure 5.6. Note that the mathematical procedure to include the effect of the bogie on the excitation of the model is not shown in the figure.

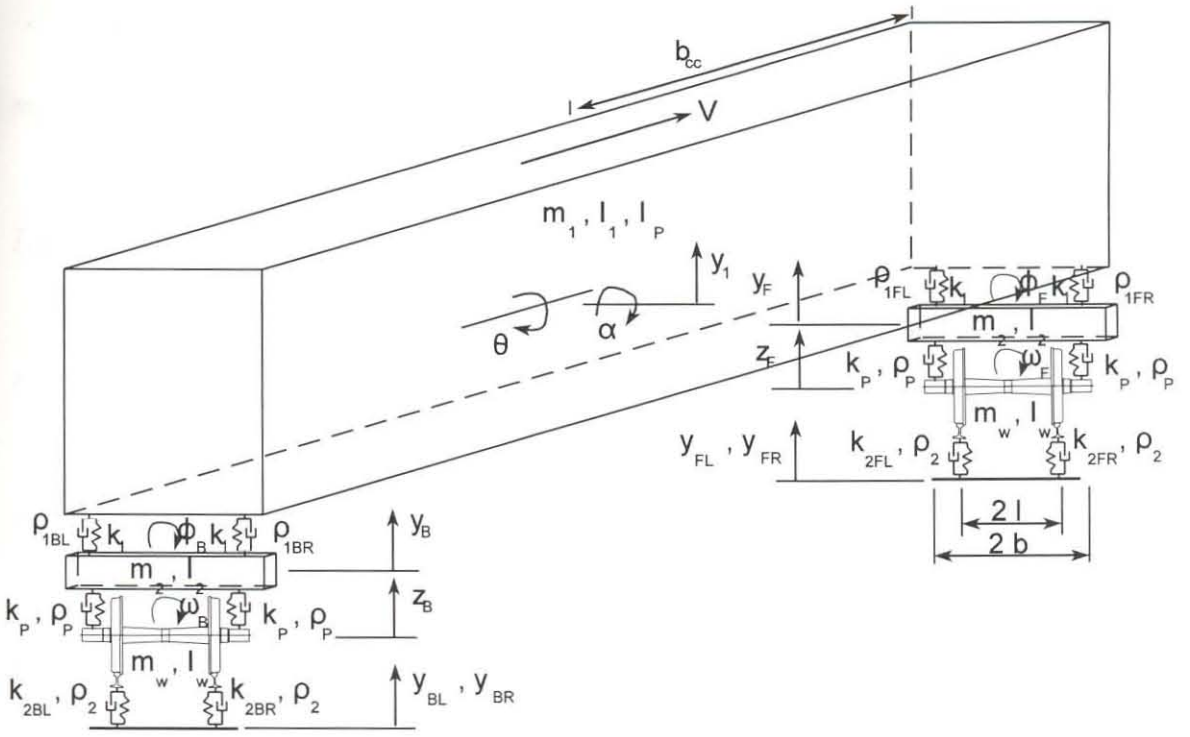

Figure 5.6: Eleven degree-of-freedom vehicle/track model.

As mentioned, all the major body modes of vibration were included to simulate the influence of track input being different at the front and the rear of the vehicle at any point in time as this has a significant influence on the dynamic behaviour of the vehicle, in particular its rolling motion, and the subsequent dynamic loading of the

track. Furthermore, the nonlinearity of the secondary suspension was included as it significantly influences the magnitude and frequency of the loading between the vehicle and the track. Equations (5.19) to (5.29) below describe the model in terms of its *equations of motion*. Note that k_2 is defined by Equation (5.10) and is a function of the static load and its position along the track.

$$m_1\ddot{y}_1 + F_{ff_{1FL}} + F_{ff_{1FR}} + F_{ff_{1BL}} + F_{ff_{1BR}} + 4k_1y_1 - 2k_1 y_F - 2k_1y_B = 0 \tag{5.19}$$

$$I_1\ddot{\theta} + bF_{ff_{1FL}} - bF_{ff_{1FR}} + bF_{ff_{1BL}} - bF_{ff_{1BR}} + 4b^2k_1\theta - 2b^2k_1\,\phi_F - 2b^2k_1\phi_B = 0 \tag{5.20}$$

$$I_p\ddot{\alpha} - b_{cc}F_{ff_{1FL}} - b_{cc}F_{ff_{1FR}} + b_{cc}F_{ff_{1BL}} + b_{cc}F_{ff_{1BR}} + 4b^2{}_{cc}k_1\alpha + 2b_{cc}k_1\,y_F - 2b_{cc}k_1y_B = 0 \tag{5.21}$$

$$m_2\ddot{y}_F - F_{ff_{1FL}} - F_{ff_{1FR}} + 2\rho_p\dot{y}_F - 2k_1(y_1 - y_F) + 2k_p(y_F - z_F) + 2k_1b_{cc}\alpha - 2\rho_p\dot{z}_F = 0 \tag{5.22}$$

$$I_2\ddot{\phi}_F - bF_{ff_{1FL}} + bF_{ff_{1FR}} + 2b^2\rho_p\dot{\phi}_F - 2bk_1(b\theta - b\phi_F) + 2b^2k_p\phi_F - 2b^2\rho_p\dot{\omega}_F - 2b^2k_p\omega_F = 0 \tag{5.23}$$

$$m_2\ddot{y}_B - F_{ff_{1BL}} - F_{ff_{1BR}} + 2\rho_p\dot{y}_B - 2k_1(y_1 - y_B) + 2k_p(y_B - z_B) - 2k_1b_{cc}\alpha - 2\rho_p\dot{z}_B = 0 \tag{5.24}$$

$$I_2\ddot{\phi}_B - bF_{ff_{1BL}} + bF_{ff_{1BR}} + 2b^2\rho_p\dot{\phi}_B - 2bk_1(b\theta - b\phi_B) + 2b^2k_p\phi_B - 2b^2\rho_p\dot{\omega}_B - 2b^2k_p\omega_B = 0 \tag{5.25}$$

$$m_w\ddot{z}_F + 2(\rho_p + \rho_2)\dot{z}_F + 2k_pz_F + k_{2FL}z_F + k_{2FR}z_F - 2\rho_p\dot{y}_F - 2k_py_F - k_{2FL}y_{FLi} - k_{2FR}y_{FRi} + k_{2FL}l\omega_F - k_{2FR}l\omega_F = 0 \tag{5.26}$$

$$I_w\ddot{\omega}_F + 2(b^2\rho_p + l^2\rho_2)\dot{\omega}_F + 2b^2k_p\omega_F + k_{2FL}l^2\omega_F + k_{2FR}l^2\omega_F - 2\rho_pb^2\dot{\phi}_F - 2k_pb^2\phi_F - k_{2FL}ly_{FLi} + k_{2FR}ly_{FRi} + k_{2FL}lz_F - k_{2FR}lz_F = 0 \tag{5.27}$$

$$m_w\ddot{z}_B + 2(\rho_p + \rho_2)\dot{z}_B + 2k_pz_B + k_{2BL}z_B + k_{2BR}z_B - 2\rho_p\dot{y}_B - 2k_py_B - k_{2BL}y_{BLi} - k_{2BR}y_{BRi} + k_{2BL}l\omega_B - k_{2BR}l\omega_B = 0 \tag{5.28}$$

$$I_w\ddot{\omega}_B + 2(b^2\rho_p + l^2\rho_2)\dot{\omega}_B + 2b^2k_p\omega_B + k_{2BL}l^2\omega_B + k_{2BR}l^2\omega_B - 2\rho_pb^2\dot{\phi}_B - 2k_pb^2\phi_B - k_{2BL}ly_{BLi} + k_{2BR}ly_{BRi} + k_{2BL}lz_B - k_{2BR}lz_B = 0 \tag{5.29}$$

with the friction forces, *Fff*, defined as follows:

$F_{ff_{FL}}$:

$$\begin{aligned}
&If\ (\dot{y}_1 - \dot{y}_F + b\dot{\theta} - b\dot{\phi}_F - b_{cc}\dot{\alpha}) < 0.0 \\
&then\quad F_{ff_{FL}} = \frac{-(x_{ss} + (y_1 - y_F + b\theta - b\phi_F - b_{cc}\alpha))\, k_{ss}\, \mu}{\tan\alpha_w + \mu} \\
&If\ (\dot{y}_1 - \dot{y}_F + b\dot{\theta} - b\dot{\phi}_F - b_{cc}\dot{\alpha}) > 0.0 \\
&then\quad F_{ff_{FL}} = \frac{(x_{ss} + (y_1 - y_F + b\theta - b\phi_F - b_{cc}\alpha))\, k_{ss}\, \mu}{\tan\alpha_w - \mu} \\
&If\ |C_{slope}(\dot{y}_1 - \dot{y}_F + b\dot{\theta} - b\dot{\phi}_F - b_{cc}\dot{\alpha})| < |F_{ff_{FL}}| \\
&then\quad F_{ff_{FL}} = C_{slope}(\dot{y}_1 - \dot{y}_F + b\dot{\theta} - b\dot{\phi}_F - b_{cc}\dot{\alpha})
\end{aligned} \tag{5.30}$$

$F_{ff_{FR}}$:

$$\begin{aligned}
&If\ (\dot{y}_1 - \dot{y}_F - b\dot{\theta} + b\dot{\phi}_F - b_{cc}\dot{\alpha}) < 0.0 \\
&then\quad F_{ff_{FR}} = \frac{-(x_{ss} + (y_1 - y_F - b\theta + b\phi_F - b_{cc}\alpha))\, k_{ss}\, \mu}{\tan\alpha_w + \mu} \\
&If\ (\dot{y}_1 - \dot{y}_F - b\dot{\theta} + b\dot{\phi}_F - b_{cc}\dot{\alpha}) > 0.0 \\
&then\quad F_{ff_{FR}} = \frac{(x_{ss} + (y_1 - y_F - b\theta + b\phi_F - b_{cc}\alpha))\, k_{ss}\, \mu}{\tan\alpha_w - \mu} \\
&If\ |C_{slope}(\dot{y}_1 - \dot{y}_F - b\dot{\theta} + b\dot{\phi}_F - b_{cc}\dot{\alpha})| < |F_{ff_{FR}}| \\
&then\quad F_{ff_{FR}} = C_{slope}(\dot{y}_1 - \dot{y}_F - b\dot{\theta} + b\dot{\phi}_F - b_{cc}\dot{\alpha})
\end{aligned} \tag{5.31}$$

$F_{ff_{BL}}$:

$$\begin{aligned}
&If\ (\dot{y}_1 - \dot{y}_B + b\dot{\theta} - b\dot{\phi}_B + b_{cc}\dot{\alpha}) < 0.0 \\
&then\quad F_{ff_{BL}} = \frac{-(x_{ss} + (y_1 - y_B + b\theta - b\phi_B + b_{cc}\alpha))\, k_{ss}\, \mu}{\tan\alpha_w + \mu} \\
&If\ (\dot{y}_1 - \dot{y}_B + b\dot{\theta} - b\dot{\phi}_B + b_{cc}\dot{\alpha}) > 0.0 \\
&then\quad F_{ff_{BL}} = \frac{(x_{ss} + (y_1 - y_B + b\theta - b\phi_B + b_{cc}\alpha))\, k_{ss}\, \mu}{\tan\alpha_w - \mu} \\
&If\ |C_{slope}(\dot{y}_1 - \dot{y}_B + b\dot{\theta} - b\dot{\phi}_B + b_{cc}\dot{\alpha})| < |F_{ff_{BL}}| \\
&then\quad F_{ff_{BL}} = C_{slope}(\dot{y}_1 - \dot{y}_B + b\dot{\theta} - b\dot{\phi}_B + b_{cc}\dot{\alpha})
\end{aligned} \tag{5.32}$$

$$
\begin{aligned}
F_{ff_{BR}}: \quad & If\ (\dot{y}_1 - \dot{y}_B - b\dot{\theta} + b\dot{\phi}_B + b_{cc}\dot{\alpha}) < 0.0 \\
& then \quad F_{ff_{BR}} = \frac{-(x_{ss} + (y_1 - y_B - b\theta + b\phi_B + b_{cc}\alpha))\, k_{ss}\, \mu}{\tan \alpha_w + \mu} \\
& If\ (\dot{y}_1 - \dot{y}_B - b\dot{\theta} + b\dot{\phi}_B b_{cc}\dot{\alpha}) > 0.0 \\
& then \quad F_{ff_{BR}} = \frac{(x_{ss} + (y_1 - y_B - b\theta + b\phi_B + b_{cc}\alpha))\, k_{ss}\, \mu}{\tan \alpha_w - \mu} \\
& If\ |C_{slope}(\dot{y}_1 - \dot{y}_B - b\dot{\theta} + b\dot{\phi}_B + b_{cc}\dot{\alpha})| < |F_{ff_{BR}}| \\
& then \quad F_{ff_{BR}} = C_{slope}(\dot{y}_1 - \dot{y}_B - b\dot{\theta} + b\dot{\phi}_B + b_{cc}\dot{\alpha})
\end{aligned}
\tag{5.33}
$$

To solve this system of equations the derivatives in the differential equations were replaced by finite central difference approximations and solved using the same technique as described in Section 5.4.1. In terms of the force between the wheel and the rail, the average force between the leading and the trailing wheel on either side of each bogie is given as output.

During the development of the vehicle/track model, a parameter variation analysis was done to evaluate the sensitivity of the vehicle/track model to changes in certain suspension parameters. In this study it was found that under the prevailing relatively good track condition, changes in the damping of the primary suspension as well as changes in the stiffness of the secondary suspension have no significant influence on the dynamic wheel load. Changes in the stiffness of the primary suspension only resulted in changes in the frequency of the dynamic wheel load. The most significant changes were observed when changing the coefficient of friction in the load dependent friction damper of the secondary suspension. An increase in the coefficient of friction resulted in a higher dynamic wheel load. From laboratory tests as described in Appendix B Section B.1.2, a realistic coefficient of friction could however be chosen to achieve realistic dynamic wheel loads.

Summary

After considering the track support model to be used and defining the type of track input, a number of alternative vehicle/track models were evaluated. The final eleven degree-of-freedom model is described in terms of its equations of motion. In Chapter 6, this model is implemented in the Dynamic Track Deterioration Prediction Model.